PHYSICAL REVIEW A **68**, 011801(R) (2003)

Transition from hexagons to optical turbulence

Damià Gomila and Pere Colet
Institut Mediterrani d'Estudis Avançats (IMEDEA, CSIC-UIB), Campus Universitat Illes Balears, E-07071 Palma de Mallorca (Balears), Spain*

(Received 8 November 2002; published 24 July 2003)

We characterize the different dynamical regimes and bifurcations in the transition from a stationary hexagonal pattern to optical turbulence. In order to characterize the bifurcations we perform linear stability analysis of stationary hexagonal patterns and Floquet analysis of oscillating hexagons. The interplay between space and time leads to a series of bifurcations showing spatial-period multiplying and quasiperiodicity.

DOI: 10.1103/PhysRevA.68.011801 PACS number(s): 42.65.Sf, 47.20.Ky, 47.54.+r, 89.75.Kd

Unlike low dimensional dynamical systems, where different scenarios for the transition to chaos have been established [1,2], in spatially extended systems the transition from regular stationary patterns to spatiotemporal chaotic regimes is only partially understood. Even the analysis of secondary instabilities of stationary patterns is not a trivial task. Some results have been obtained either using amplitude equations [3] or symmetry-based approaches [4–6]. In the first case amplitude equations are obtained close to the primary instability, leading to the formation of the pattern, therefore only secondary bifurcations close to this point can be analyzed. The second is a very powerful mathematical technique that classifies the different ways in which the spatial symmetry can be broken, however, it does not discriminate which one will take place in a specific system. More detailed analysis can be carried out in coupled map lattices [7], where a simultaneous period and wavelength doubling route to spatiotemporal chaos has been reported.

Experimentally, secondary bifurcations of stationary hexagonal patterns have been observed in a sodium cell with a single feedback mirror [8] leading to stationary quasipatterns and superlattices, in liquid-crystal light valves leading to stationary superlattices [9] and chaotic structures [10], and in hydrodynamic systems [11] leading to stationary superlattices. Instabilities of one-dimensional (1D) oscillatory patterns that give rise to additional wave components have been observed in liquid-crystal light valves [12].

In this paper we analyze the role of the spatial degrees of freedom in the transition from a stationary hexagonal pattern to chaotic hexagons and turbulence in a prototypical nonlinear optical model. In order to characterize different instabilities we perform semianalytical linear stability analysis of stationary hexagonal patterns and more important, Floquet analysis of oscillatory hexagonal superlattices.

We consider a ring optical cavity filled with a self-focusing Kerr medium and pumped by an external field E_0. In the mean-field approximation, the transverse dynamics of the slowly varying electric-field envelope $E(\vec{x},t)$ is given by [13]

$$\partial_t E = -(1+i\theta)E + i\nabla^2 E + E_0 + i2|E|^2 E, \tag{1}$$

where θ is the cavity detuning and ∇^2 the transverse Laplacian. The homogeneous steady-state solution is given implicitly by $E_0 = E_s[1-i(2I_s-\theta)]$, where $I_s \equiv |E_s|^2$. This solution presents bistability for $\theta > \sqrt{3}$. We will restrict ourselves to the nonbistable regime $\theta < \sqrt{3}$. We consider I_s, directly related with E_0 by the previous implicit equation, as the control parameter. A linear stability analysis with respect to spatially periodic perturbations yields [14,15]

$$\sigma(k) = -1 \pm \sqrt{(\theta + k^2 - 6I_s)(2I_s - \theta - k^2)}, \tag{2}$$

where $\sigma(k)$ is the linear growth rate of a perturbation with wave vector $\vec{k}$ and $k = |\vec{k}|$. The instability threshold is located at $I_s^c = 1/2$ and the critical wave number is $k_c = \sqrt{2-\theta}$. For $I_s > I_s^c$, the maximum linear growth rate is for wave vectors with $k_u = \sqrt{4I_s - \theta}$. Starting from the homogeneous solution and increasing the pump intensity to a value above, but close to, threshold, a hexagonal pattern with a wave number k close to k_u arises subcritically [14,15]. Typically, this pattern oscillates even just above threshold [14,16]. The amplitude of the oscillations decreases with decreasing I_s until it becomes stationary. Figure 1(a) shows a stationary hexagonal pattern for $\theta = 1$ with wavelength $\lambda_1 = 2\pi/k_h$ and $k_h = 1.15k_c$ at $I_s = 0.46$, which is stable until $I_s = 0.45$ where it decays to the homogeneous solution [17]. It was initially a nonstationary pattern formed at $I_s = 1.16 I_s^c$ (for which $k_u = 1.15k_c$).

The stationary hexagonal pattern can be written as

$$E_h(\vec{x}) = \sum_{n=0}^{N} a_n e^{i\vec{k}_n^0 \cdot \vec{x}}, \tag{3}$$

where a_n are complex coefficients, $\vec{k}_0^0$ is the homogeneous mode, and $\vec{k}_n^0$ ($n = 1, \ldots, 6$) are the fundamental modes of the hexagonal pattern with modulus k_h. As this is a subcritical pattern, even at threshold, harmonics have a finite size, which is enhanced by the Kerr self-focusing effect. Therefore, we take into account up to the $5k_h$ ($\vec{k}_n^0$ for $n = 7, \ldots, N = 90$) harmonics.

Linearizing Eq. (1) around stationary pattern (3), we obtain for $\delta E(\vec{x},t) = E(\vec{x},t) - E_h(\vec{x})$ [18]

*URL: http://www.imedea.uib.es/PhysDept

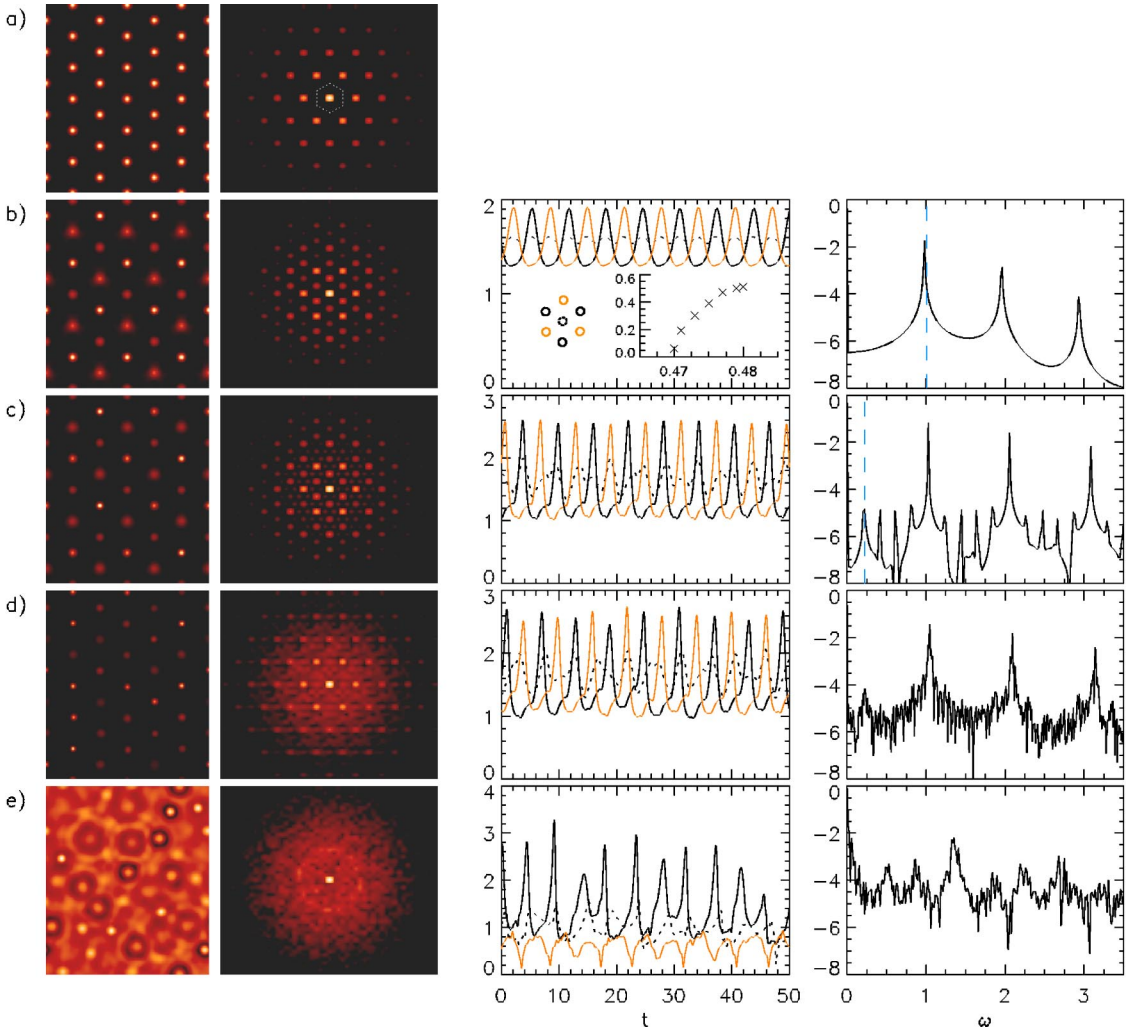

FIG. 1. Spatiotemporal regimes of a hexagonal pattern obtained from numerical integration of Eq. (1) [17]. From top to bottom: stationary ($I_s=0.46$), periodic ($I_s=0.48$), quasiperiodic ($I_s=0.525$), chaotic ($I_s=0.54$), and spatiotemporal chaos ($I_s=0.62$). From left to right: $|E(\vec{x})|^2$, $|E(\vec{k})|^2$, time evolution of three hexagonal peaks (see text), and power spectra corresponding to the time trace plotted with a black solid line. The vertical dashed lines in the last column of rows (b) and (c) indicate predicted frequencies ω_1 and ω_2.

$$\partial_t \delta E = -(1+i\theta)\delta E + i\nabla^2 \delta E + i2[2|E_h|^2 \delta E + E_h^2 \delta E^*], \tag{4}$$

where the linear operator of the right-hand side has periodic coefficients. Its eigenfunctions $\psi(\vec{x},\vec{q})$ can be written in a Bloch form [4]:

$$\psi(\vec{x},\vec{q}) = e^{i\vec{q}\cdot\vec{x}} A(\vec{q},\vec{x}), \tag{5}$$

where $A(\vec{q},\vec{x})$ is a function with the same periodicity as pattern $E_h(\vec{x})$ and therefore, it can be written as $A(\vec{q},\vec{x}) = \Sigma_{n=0}^{N} \alpha_n(\vec{q}) e^{i\vec{k}_n^0\cdot\vec{x}}$. The stability of E_h reduces then to the study of the eigenvalue problem for coefficients $\alpha_n(\vec{q},t)$ obtained from Eqs. (4) and (5) [18]:

$$M(a_n,\vec{q})\vec{\Sigma}(\vec{q}) = \sigma\vec{\Sigma}(\vec{q}), \tag{6}$$

with $\vec{\Sigma}(\vec{q}) \equiv (\alpha_0(\vec{q}), \ldots, \alpha_N(\vec{q}), \alpha_0^*(-\vec{q}), \ldots, \alpha_N^*(-\vec{q}))^T$. Note that eigenfunctions with different $\vec{q}$ are uncoupled, except those with $\vec{q}$ and $-\vec{q}$, due to the coupling of δE with δE^* in Eq. (4). To know the stability of the solution it is sufficient to consider only vectors $\vec{q}$ inside the first Brillouin zone of the hexagonal lattice defined by wave vectors $\vec{k}_n^0$ of pattern in Fig. 1(a). In fact, due to the hexagonal symmetry it is sufficient to consider only 1/6 of the first Brillouin zone. The $2N$ eigenvalues $\sigma_i(\vec{q})$ of matrix $M(a_n,\vec{q})$ determine the stability of the pattern against perturbations with wave vectors $\vec{k}_n^0 \pm \vec{q}$. Due to the symmetries of M, these eigenvalues are either real or complex conjugates. We order $\sigma_i(\vec{q})$ as $\mathrm{Re}[\sigma_i(\vec{q})] \geqslant \mathrm{Re}[\sigma_{i+1}(\vec{q})]$.

For $0.45 < I_s < 0.47$, all the eigenvalues have negative real part, except for two zero eigenvalues corresponding to the neutral modes associated with the translational invariance (Goldstone modes) [18,19], so the stationary hexagonal pattern is stable. For $I_1 = 0.470$, the hexagons undergo a finite wavelength Hopf bifurcation (Fig. 2). The unstable mode has a wave vector $\vec{q}_1 = (\vec{k}_1^0 + \vec{k}_2^0)/3$ located on the vertex of the

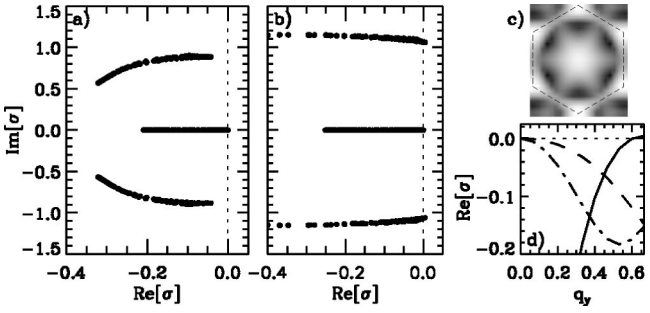

FIG. 2. Largest eigenvalues of the stationary hexagonal pattern obtained solving Eq. (6). (a) Below the Hopf instability ($I_s = 0.46$). (b) Just above the Hopf unstability ($I_s = 0.48$). (c) Re$[\sigma_0(q_x, q_y)]$ for $I_s = 0.48$. The dashed hexagon indicates the first Brillouin zone. (d) Transverse cut of Re$[\sigma_0(q_x, q_y)]$ along the q_y axis.

first Brillouin zone ($|\vec{q}_1| = k_h/\sqrt{3}$). As a consequence, hexagons do not oscillate uniformly, instead, they are divided in three superlattices of wavelength $\lambda_1 = \sqrt{3}\lambda_h$ corresponding to the unstable eigenmode. The peaks in each superlattice oscillate synchronously. Two of the superlattices oscillate in antiphase at frequency $\omega_1 = \mathrm{Im}[\sigma_0(\vec{q}_1)] = 1.062$ with a relatively large amplitude while the third oscillates at twice that frequency and has a smaller amplitude [Fig. 1(b)]. Physically, this reflects an exchange of energy between two of the superlattices, mediated by the third while the total energy remains practically constant. The high Fourier harmonics play an important role in these oscillations. Neglecting or filtering out successive rings of high harmonics shifts the bifurcation to larger values of the pump intensity and may eventually suppress the bifurcation altogether [20]. Therefore, this oscillation is associated with an energy transfer from large scales to small scales. The bifurcation is supercritical; close to I_1, amplitude of the oscillations grows as $\sqrt{I_s - I_1}$, as shown in the inset of the third column of Fig. 1(b). Mathematically, this bifurcation is a spatial-period multiplying [6]. Stationary instabilities with the same wave vector $\vec{q}_1$ have been observed in surface waves [11] leading to superlattices.

We next analyze the stability of the periodically oscillating hexagons. This limit cycle solution of Eq. (1) can be written in form (3) with time-periodic coefficients $a_n(t + T_1) = a_n(t)$, where $T_1 = 2\pi/\omega_1$. Including all the Fourier modes that have been excited in the previous bifurcation up to $5k_h$ we have $N = 369$. Coefficients $\alpha_n(\vec{q})$ are now time dependent $\alpha_n(\vec{q}, t)$ and its evolution is given by a set of linear differential equations with time-periodic coefficients

$$\partial_t \vec{\Sigma}(\vec{q}, t) = M(a_n(t), \vec{q})\vec{\Sigma}(\vec{q}, t). \tag{7}$$

So, by the Floquet theorem the general solution has the form

$$\vec{\Sigma}(\vec{q}, t) = \vec{\Sigma}(\vec{q}, 0)P(t)e^{\Lambda(\vec{q})t}, \tag{8}$$

where $P(t)$ is a period-T_1 matrix and $\Lambda(\vec{q})$ is a time-independent matrix. The limit cycle is numerically determined from Eq. (1) and matrix $e^{\Lambda(\vec{q})T_1}$ is computed integrating Eq. (8) over period T_1 [21]. Its $2N$ eigenvalues (Floquet multipliers) $m_j(\vec{q})$ determine the stability of the oscillating hexagons under any possible perturbation with wave vectors $\vec{k}_n^0 \pm \vec{q}$. It is sufficient to explore 1/6 of the first Brillouin zone of the hexagonal lattice in Fourier space whose fundamental wave vectors now have a modulus $k_h/\sqrt{3}$.

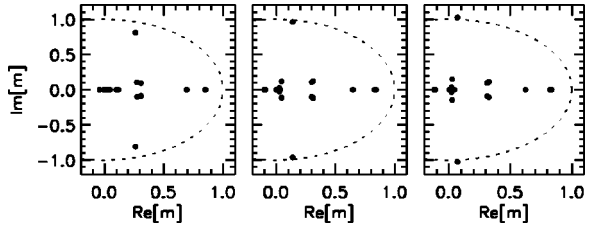

FIG. 3. Floquet multipliers for perturbations with $\vec{q} = \vec{q}_2$ for (from left to right) $I_s = 0.51, 0.52$, and 0.525.

For pump intensities $0.470 < I_s < 0.523$, all the Floquet multipliers (except the one corresponding to the neutral mode) have modulus smaller than one and therefore, the oscillating hexagons are stable. For $I_s = 0.523$ there is a couple of complex conjugate Floquet multipliers with nonvanishing imaginary part, which crosses the unit circle (Fig. 3). This Neimark-Sacker bifurcation [2] introduces a temporal frequency $\omega_2 = \mathrm{Im}[\ln(m_0(\vec{q}_2))]/T_1 = 0.220$ and therefore, the temporal behavior will be quasiperiodic. The frequency predicted from the Floquet analysis is in very good agreement with the second frequency present in the quasiperiodic time series obtained from numerical simulations of Eq. (1) [Fig. 1(c)]. The unstable mode has a wave vector located at the vertex of Brillouin zone $\vec{q}_2 = (\vec{k}_1^0 + \vec{k}_2^0)/3$, $\vec{k}_{1,2}^0$ being fundamental wave vectors of this lattice. Since the fundamental wave vectors have now a modulus $k_h/\sqrt{3}$, $|\vec{q}_2| = k_h/3$. Thus, this second bifurcation introduces a characteristic wavelength $\lambda_2 = \sqrt{3}\lambda_1 = 3\lambda_h$ [Fig. 1(c)]. At this point, the solution the system displays has three characteristic spatial wavelengths and two temporal frequencies. The spatial structure of this series of bifurcations is equivalent, in hexagonal patterns, to the wavelength doubling bifurcations found in 1D systems [7]. The temporal behavior, however, does not correspond to period doubling but to a quasiperiodic route [1].

The quasiperiodic oscillating hexagons are stable for pump intensities $0.523 < I_s \lesssim 0.528$. Note that the parameter range between successive bifurcations decreases. Numerical simulations done for different system sizes, including very large systems, indicate that the quasiperiodic hexagons become unstable for $I_s \sim 0.528$. A close inspection to the far field shows that the system becomes unstable against long-wavelength perturbations. A continuous of small wave vectors ($q \sim 0$) grow and the whole background of Fourier modes become excited [Fig. 1(d)]. Peaks are still located on a hexagonal lattice but the spatial structure of the oscillations is lost, so this is a regime of spatiotemporal chaos on top of a hexagonal lattice. The continuous of excited Fourier modes have a continuous of associated temporal frequencies that make the oscillations of the peaks temporally chaotic, showing a broadband power spectrum [Fig. 1(d)]. The temporal

behavior of the system shows a quasiperiodic route to chaos [1], namely, a chaotic regime is observed after the instability of a torus. In the study of these routes the spatial dependence is not considered but as we show here, it plays a very important role in extended systems. We have shown that each bifurcation introduces it's own spatial wavelength, making the system spatially more complicated. Chaotic hexagons are observed in quite a broad parameter range ($0.528 \lesssim I_s \lesssim 0.62$).

Finally, for pump intensities above $I_s \sim 0.62$ a sudden change occurs. The spatial order is completely lost and all the Fourier modes with wave number close to k_u become equally excited [Fig. 1(e)]. This is a regime of spatiotemporal chaos where peaks at random positions grow and decay, producing circular waves that propagate in the transverse plane and dissipate away [22], a behavior somehow like in Langmuir turbulence in plasma [23]. Equation (1) is, in fact, a modified nonlinear Schrödinger equation and the phenomenon of wave collapse [24] is behind the oscillation of the peaks in our system [22]. Collapse is prevented by losses [25]. This regime of optical turbulence is, for large values of the pump intensity, the attractor of the dynamics starting from random initial condition. In fact, it was already an attractor of the dynamics for lower values of the pump intensity, coexisting with the chaotic hexagons. The sudden instability of the chaotic hexagons may correspond to a crisis [1] caused by the collision of the chaotic attractor with an unstable manifold. In extended systems, a crisis has been found in a 1D system [26], where a temporally chaotic state leads to a spatiotemporal chaos regime due to a resonance with an unstable solution.

In summary, we have analyzed the transition from a stationary hexagonal pattern to chaotic hexagons and turbulence in the transverse plane of a prototypical nonlinear optical model. Stability analysis of both stationary and oscillatory hexagonal structures proves the existence of a Hopf bifurcation associated with a subdivision of the hexagonal structure in three superlattices and a subsequent Neimark-Sacker bifurcation that introduces another temporal frequency and a division in three, of each of the superlattices. Chaos appears through a long-wavelength instability, which is present only in extended systems. This instability leads to a spatiotemporal chaotic regime in which peaks are still located on a hexagonal lattice. Finally, spatial order is completely lost after a subsequent instability and the system enters in a regime of optical turbulence. We expect the scenario presented here to be relevant for systems displaying hexagonal patterns whose peaks undergo oscillatory instabilities. Also, the sequence of transitions up to chaotic hexagons can be relevant for hexagonal lattices of coupled oscillators.

The authors acknowledge helpful discussions with M. San Miguel, E. Hernández-García, O. Piro, M. Matias, and M. Santagiustina, and financial support from the MCyT (Spain, Project Nos. PB97-0141-C02-02, BFM2000-1108, and BFM2001-0341-C02-02).

[1] P. Berge, Y. Pomeau, and C. Vidal, *Order within Chaos* (Wiley, New York, 1984); P. Manneville, *Dissipative Structures and Weak Turbulence* (Academic, Boston, 1990); E. Ott, *Chaos in Dynamical Systems* (Cambridge University, Cambridge, 1993).

[2] Y.A. Kuznetsov, *Elements of Applied Bifurcation Theory* (Springer-Verlag, New York, 1995).

[3] D. Walgraef, *Spatio-Temporal Pattern Formation* (Springer-Verlag, New York, 1997).

[4] P. Coullet and G. Iooss, Phys. Rev. Lett. **64**, 866 (1990).

[5] B. Dionne, M. Silber, and A.C. Skeldom, Nonlinearity **10**, 321 (1997).

[6] D.P. Tse *et al.*, Physica D **146**, 367 (2000).

[7] R.E. Amritkar and P.M. Gade, Phys. Rev. Lett. **70**, 3408 (1993).

[8] R. Herrero *et al.*, Phys. Rev. Lett. **82**, 4627 (1999); E. Grosse Westhoff *et al.*, Phys. Rev. E **67**, 025203 (2003).

[9] E. Pampaloni *et al.*, Phys. Rev. Lett. **78**, 1042 (1997).

[10] F. Castaldo, D. Paparo, and E. Santamato, Opt. Commun. **143**, 57 (1997).

[11] A. Kudrolli, B. Pier, and J.P. Gollub, Physica D **123**, 99 (1998); C. Wagner, H.W. Müller, and K. Knorr, Phys. Rev. Lett. **83**, 308 (1999); H.J. Pi *et al.*, *ibid.* **84**, 5316 (2000); J.L. Rogers *et al.*, *ibid.* **85**, 4281 (2000).

[12] S. Residori, A. Petrossian, and L. Gil, Phys. Rev. Lett. **88**, 233901 (2002).

[13] L.A. Lugiato and R. Lefever, Phys. Rev. Lett. **58**, 2209 (1987).

[14] A.J. Scroggie *et al.*, Chaos, Solitons Fractals **4**, 1323 (1994).

[15] M. Tlidi, R. Lefever, and P. Mandel, Quantum Semiclassic. Opt. **8**, 931 (1996).

[16] M. Hoyuelos *et al.*, Phys. Rev. E **58**, 2992 (1998).

[17] We integrate Eq. (1) using a pseudospectral method as in R. Montagne *et al.*, Phys. Rev. E **56**, 151 (1997). Linear terms in Fourier space are treated exactly while a second-order in time approximation is used for nonlinear terms. We use a 512 $\times$512 rectangular grid with $\Delta k_x = k_h/6$ and $\Delta k_y = \sin(60°)\Delta k_x$ such that the hexagonal pattern wave vectors lie on the lattice.

[18] D. Gomila and P. Colet, Phys. Rev. E **66**, 046223 (2002).

[19] D. Foster, *Hydrodynamic Fluctuations, Broken Symmetry and Correlation Functions* (Addison Wesley, Redwood City, 1983).

[20] M. Le Berre *et al.*, Phys. Rev. A **56**, 3150 (1997); G. Harkness *et al.*, *ibid.* **58**, 2577 (1998); A.V. Mamaev and M. Saffman, Phys. Rev. Lett. **80**, 3499 (1998).

[21] J.H.E. Cartwright, E. Hernández-García, and O. Piro, Phys. Rev. Lett. **79**, 527 (1997).

[22] A.C. Newell, D.A. Rand, and D. Russell, Phys. Lett. A **132**, 112 (1988).

[23] P.A. Robinson, Rev. Mod. Phys. **69**, 507 (1997).

[24] J.J. Rasmussen and K. Rypdal, Phys. Scr. **33**, 481 (1986); L. Berg, Phys. Rep. **303**, 259 (1998).

[25] M.V. Goldman, K. Rypdal, and B. Hafizi, Phys. Fluids **23**, 945 (1980).

[26] K. He, Phys. Rev. Lett. **84**, 3290 (2000).